^{13}C NMR Investigation of Molecular Chain Diffusion in Semicrystalline Polyethylene. 1. Effect of Cross-Linking

Malcolm B. Robertson,† Ian M. Ward, and Philip G. Klein*

IRC in Polymer Science and Technology, University of Leeds, Leeds LS2 9JT, U.K.

Kenneth J. Packer

Department of Physical Chemistry, Nottingham University, Nottingham, NG7 2RD, U.K.

Received June 16, 1997; Revised Manuscript Received August 28, 1997[⊗]

ABSTRACT: Solid-state molecular chain diffusion in linear high-density polyethylene (HDPE) is established as the dominant mechanism for the crystalline ^{13}C longitudinal relaxation at 60 °C, confirming previous work of Schmidt-Rohr and Spiess. A progressive saturation NMR experiment was undertaken on several samples of HDPE, where different degrees of cross-linking were introduced by electron irradiation. A decrease in the rate of recovery of the crystalline signal was observed with an increase in cross-link density, as measured by gel fraction. As irradiation forms cross-links on the fold surfaces of the lamellae, this behavior cannot be explained through a conventional dipolar spin−lattice mechanism or ^{13}C spin diffusion. Transport of magnetization via chain diffusion to the amorphous region, where it experiences an efficient relaxation process, is consistent with the relaxation data and the Overhauser enhancement. As the gel fraction increased from zero to 87%, the effective diffusion coefficients almost halved from the nonirradiated sample (0.033 $nm^2 \cdot s^{-1}$) to 0.018 $nm^2 \cdot s^{-1}$.

Introduction

The earliest investigations of the ^{13}C longitudinal relaxation in polyethylene,[1−4] assumed that the origin of the relaxation was a simple spin−lattice process, where nuclei experienced the same mobility throughout the bulk of the crystal. The initial part of the decay was observed to be non-exponential, which was attributed to a distribution of relaxation times[5] or the possibility of spin-diffusion within the crystalline regions.[6] The complete relaxation required a multiexponential model to satisfactorily represent the data. However, it was then necessary to postulate the number of components without either an adequate morphological nor dynamical model.

Although the crystalline carbons experience the same molecular environment, within the crystallites, the single exponential fits to the longitudinal relaxation associated with the crystal phase encompass a surprisingly wide range of times. Lamellar thickness has been identified as the principal structural variable in determining the time scale of the relaxation, the T_1 of the crystal phase being proportional to the lamellar thickness. A mechanism to account for this dependence has been proposed,[7] namely transport of ^{13}C magnetization between the crystalline and amorphous regions. A self-consistent pattern was established which indicated that the ^{13}C relaxation was influenced by the same factors as the spin diffusion model for ^{1}H T_1 relaxation. However, doubts were raised concerning the validity of natural abundance ^{13}C spin diffusion, as the sole transport mechanism.

More recently, a series of longitudinal relaxation measurements in polyethylene has been interpreted by Schmidt-Rohr and Spiess[8] as long distance solid-state chain diffusion between the amorphous and crystalline regions. Two-dimensional exchange NMR and nuclear Overhauser enhancement measurements supported these conclusions. The proposed mechanism for this transport was assigned to a chain jump process, first presented as a mechanism for the relaxation observed by dynamic mechanical spectroscopy.[9] This relationship between the process and longitudinal relaxation was already well established.[6] However, the employment of the multiple component spin−lattice relaxation model in subsequent publications[10,11] indicates that the chain diffusion interpretation is not yet universally accepted. The aim of the present investigation is to clarify the origin of the ^{13}C longitudinal relaxation and relate it to the structure of polyethylene.

Topological constraints, e.g., entanglements, branching, and cross-linking, should hinder the diffusion mechanism, while their effect on a classical dipolar spin−lattice relaxation process should be negligible. It has been established that electron beam irradiation of solid polyethylene produces cross-links predominantly on the crystal fold surfaces, while cross-links are virtually absent from the crystallite interior.[12,13] Under these circumstances, the motion present in the crystal, which is required for spin−lattice relaxation, should be largely unaffected by the cross-links. However, if the origin of the longitudinal relaxation is molecular chain diffusion, an increase in the relaxation time scale should be observed on cross-linking the polymer chains. In this paper, the ^{13}C longitudinal relaxation is measured for polyethylene samples containing controlled amounts of radiation-induced cross-linking.

Experimental Section

Sample Preparation. The polyethylene used was a slow-cooled, high-density material which was processed from Rigidex 006-60, of weight-average molecular weight 126 000. An isotropic block was molded from a melt of the polymer granules. Subsequently, the polyethylene was held in the mold at 110 °C for 5 h and then allowed to cool to ambient conditions.

Crosslinking of the polyethylene was performed using procedures developed at Leeds.[13] A Van de Graaf generator produced a 2.9 MeV continuous electron beam, which irradiated the samples to various doses. All samples were irradiated in an acetylene atmosphere, at atmospheric pressure, to

† Present address: Department of Physical Chemistry, Nottingham University, Nottingham NG7 2RD, U.K.

[⊗] Abstract published in *Advance ACS Abstracts,* October 15, 1997.

S0024-9297(97)00871-1 CCC: $14.00

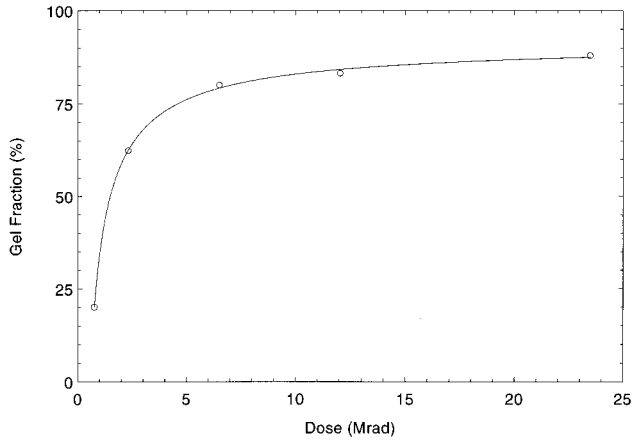

Figure 1. Gel fraction vs irradiation dose.

Table 1. Irradiation Dose−Gel Fraction Relationship

irradiation dose (Mrad)	irradiation atm	gel fraction (interpolated)
0		0
5.91	C_2H_2	0.78
22.94	C_2H_2	0.87

enhance the efficiency of the cross-linking process. Acetylene radicals diffuse into the amorphous and interfacial regions, enhancing cross-linking and considerably reducing the amount of chain scission.[14] Following the irradiation, the samples were annealed at 100 °C for 1 h, to ensure complete reaction of the radicals.

Polyethylene becomes insoluble as a consequence of cross-links between chains, which results in the formation of an insoluble network. As the technique to calculate the gel fraction (weight fraction of insoluble material) is destructive, the dependence of the gel fraction on the irradiation dose was examined on a separate set of samples to those actually used for the NMR study. The gel fraction was determined as the weight fraction of insoluble material in refluxing decalin, using standard methods.[13] Gel content initially increased rapidly with dose, indicating the introduction of cross-links between chains (Figure 1).

Subsequent irradiation produces cross-links between chains which were already joined together and therefore had a less pronounced affect on the gel fraction. As the gel fraction at the highest irradiation doses continued to increase, the rate of chain scission did not exceed that of cross-linking. Thus, the increased irradiation leads directly to a higher cross-link density.

Three polyethylene samples were then irradiated to differing extents to examine the affect of cross-link density on the ^{13}C longitudinal relaxation behavior. Electron irradiation doses were chosen to highlight the differences in cross-link density, where the gel fraction was estimated through interpolation of the existing data (Table 1). The nonirradiated sample was annealed at 100 °C for 1 h in vacuum to ensure its identical thermal history.

High-Resolution ^{13}C NMR. Spectra were recorded on a Chemagnetics CMX-200, operating at 200 MHz for protons and 50.3 MHz for carbons. A progressive saturation experiment was devised, incorporating a nuclear Overhauser enhanced pulse sequence throughout the recycle delay (Figure 2). A double resonance MAS probe was used, and samples were spun at about 3.5 kHz. A 4 μs 90° pulse was used in the ^1H and ^{13}C channels, with a decoupling field strength equivalent to 82 kHz applied during the acquisition period. A series of FIDs were recorded, with a variation in the recycle delay time, between 2 and 1200 s. All experiments were performed at 60 °C, as this temperature was believed to represent the ideal conditions for the observation of chain diffusion.[8]

The data lengths of the FIDs were doubled by zero filling[15] and then Fourier transformed into the frequency domain, where there were baseline corrected to a third-order polynomial.

Wideline ^1H NMR. The probe had a 5 mm coil, and a 90° pulse width of 2 μs was used. A standard $90_x-\tau-90_y$ solid echo pulse sequence was used, with interpulse spacing, τ, varying between 7 and 30 μs. The broad component of the spectrum (representing the crystalline phase) obtained at each value of τ was fitted to a modified Gaussian function, eq 1. Typical

$$y = a \exp(-\nu/b)^g \quad (1)$$

values of b and g were 35 kHz and 3.7, respectively. The narrow component of the spectrum, relating to the amorphous phase, was eliminated from the fit. This was done by taking the turning points in the derivative spectrum on each side of the center, and rejecting the data between these points. The fraction of the broad component as a function of decayed in a Gaussian manner, and this was extrapolated back to zero to obtain the crystallinity, which was calculated to be 77%.

Nuclear Overhauser Enhancement (NOE).[16,17] The NOE for both peaks was measured directly from the ^{13}C spectra, recorded with and without the ^1H pulse train during the recycle delay. The crystal resonance was modeled by a Lorentzian line shape with the extreme upfield part of the peak excluded from the data, as this largely eliminated the influence of the amorphous resonance on the crystal line shape. The intensity of the amorphous resonance was then calculated from the difference between the integrated area of the spectrum and the area of the fitted crystal resonance.

Results and Discussion

Nuclear Overhauser Enhancement. Comparatively low values for the NOE were recorded for all samples at the shortest recycle delay times (Figure 3). However, this behavior was a consequence of a transient nuclear Overhauser enhancement created by the saturation of the protons during the decoupling pulse, and is therefore present in the experiment without the saturating ^1H pulse train.

The enhancement reaches an asymptotic limit at longer times. The NOE generated was approximately 2.2, which was found to be invariant of the cross-link density and equal for both the crystal and amorphous resonances. The fact that the enhancements are equivalent strongly indicates that the mechanism for the longitudinal relaxation is not only similar for both phases, but independent of the cross-linking between the polyethylene chains. When the present Overhauser enhancements are compared to previous measurements[8] at $\mathbf{B}_0 = 7.05$ T, where the NOE was measured as 2.0 (in both crystalline and amorphous phases, also), it demonstrates a dependence on the static magnetic field. It is therefore doubtful that the motion creating the Overhauser enhancement is in the extreme narrowing limit. Although unlikely, other relaxation mechanisms might contribute to the enhancement, and lower its efficiency. If a single correlation time for the molecular reorientation is assumed, a maximum correlation time can be determined as $\tau_R \leq 7.6 \times 10^{-10}$ s. In actuality multiple independent motions described through distinct correlation times probably most accurately model the reorientation for a molecule with a highly anisotropic molecular structure, such as a macromolecule. However, deviation from the isotropic enhancement was shown to only occur when the correlation times for these other types of reorientation approach the extreme narrowing limit.[18]

Origin of ^{13}C Longitudinal Relaxation. The absorption intensity of the amorphous resonance, at 31.5 ppm, remains approximately constant, for the complete range of recycle delay times (Figure 4). This demonstrates that the amorphous magnetization is fully

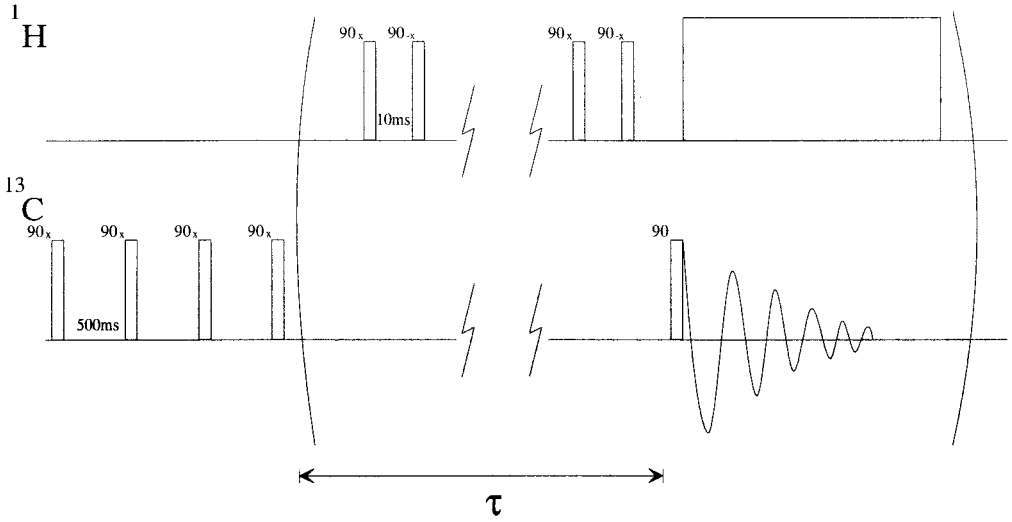

Figure 2. Progressive saturation pulse sequence developed to measure the ^{13}C longitudinal relaxation. Presaturation was performed on the ^{13}C channel before the experiment was repeated to provide a satisfactory signal to noise ratio. A nuclear Overhauser enhancement was created during the recycle delay, through saturation on the ^{1}H channel.

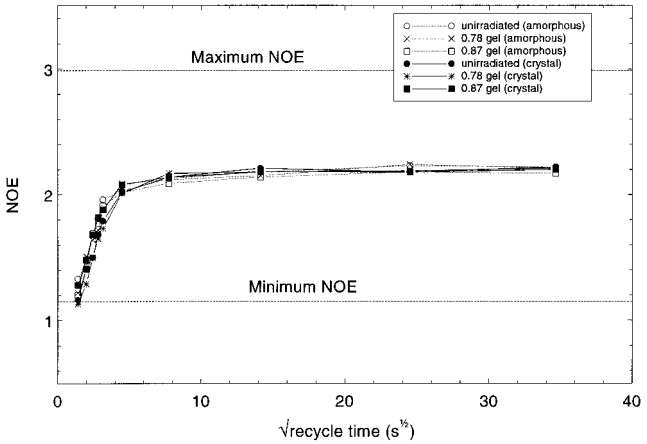

Figure 3. NOE, for all samples, as a function of the recycle delay, showing a quick convergence to an asymptotic value. Data are presented as a $t^{1/2}$ plot, which allows a clear presentation of the complete data set.

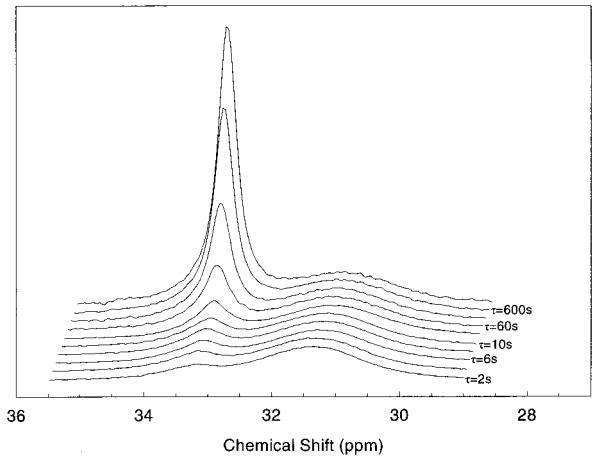

Figure 4. ^{13}C NMR spectra, at various recycle delays, as indicated, for the unirradiated sample. The enhancement with time of the crystalline resonance, at 33 ppm, occurs over several hundred seconds, while the amorphous resonance is fully relaxed within 2 s.

relaxed within two seconds (the shortest recycle delay time, τ). In contrast the crystalline signal, at 33 ppm, increases in intensity over the complete range of recycle times. This slow growth in intensity indicates that the crystal phase takes a prolonged time to recover its equilibrium magnetization.

The invariance of the amorphous signal in the ^{13}C NMR spectrum is used as a reference to calculate the growth in the intensity of the crystalline resonance. The evolution of magnetization can be represented as a fraction of the maximum crystal signal:

$$\frac{M(\tau)}{M_0} = \frac{I(\tau)}{I(\infty)} = \frac{f_C(\tau) \int S(\omega, \tau)\, d\omega}{f_C(\infty) \int S(\omega, \infty)\, d\omega} \qquad (2)$$

Here, M(τ) is the longitudinal magnetization at time τ, M_0 is the equilibrium magnetization, I(τ) is the intensity of the crystal resonance, $f_C(\tau)$ is the fraction of the crystal resonance in the ^{13}C spectrum, and $S(\omega,\tau)$ is the line shape of the total spectrum recorded at time τ.

As the amorphous resonance demonstrates complete longitudinal relaxation at the shortest recycle delay time, τ, the absolute intensity of this signal is equivalent to the signal measured at infinite time. The fraction of the crystal resonance, in the ^{13}C spectrum at infinite time, was assumed to be equivalent to the crystallinity, $F_C{}^H$, as measured by a deconvolution of the ^{1}H wide line spectrum. Figure 5 shows the wide line ^{1}H spectra for two samples, one unirradiated and the other irradiated with the maximum dose of 23 Mrad. The two spectra are virtually identical, showing that the crystallinity is unaffected by electron irradiation of these doses. The signal from the crystal phase has been fitted in Figure 5 to a modified Gaussian,[19] using the data in the wings of the spectrum, and eliminating the narrow, amorphous peak. Again, it can be seen that the area under the modified Gaussian is the same in both cases, indicating constant crystallinity. By back-extrapolation of the modified Gaussian area (see Experimental Section), this crystallinity has been calculated at 77%.

The evolution of the longitudinal magnetization can now be represented as

$$\frac{M(\tau)}{M_0} = \frac{f_C(\tau)}{1 - f_C(\tau)} \frac{1 - F_C{}^H}{F_C{}^H} \qquad (3)$$

Differences in the time scale of the longitudinal relaxation are shown between polyethylene samples

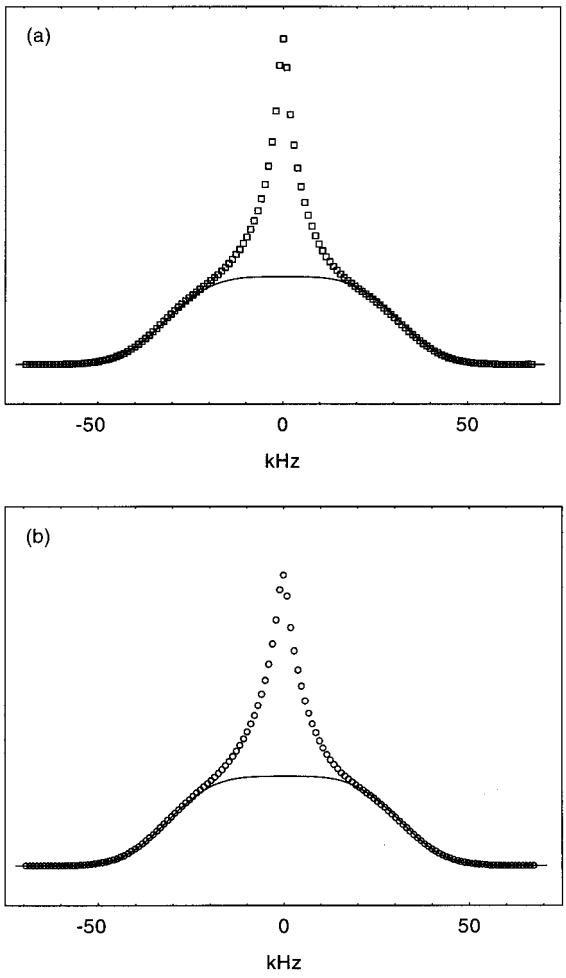

Figure 5. Wide-line ^{1}H NMR spectra, for the unirradiated sample (a), and the sample irradiated with 23 Mrad (87% gel), (b). A solid-echo pulse sequence was used, with an interpulse delay of 12 μs. The solid line is a fit to a modified Gaussian, giving a crystallinity of 70% in each case.

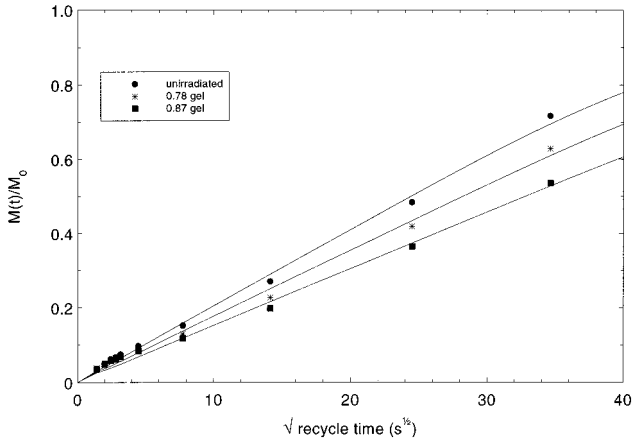

Figure 6. Fractional recovery of the crystalline peak, against $t^{1/2}$, for various samples, as indicated. The lines through the data are fits to the diffusion model, eq 4.

(Figure 6). The relaxation shows an explicit dependence on the cross-link density, which was established from the electron irradiation dose. The nonirradiated polyethylene exhibits the fastest longitudinal relaxation, while the sample with the highest irradiation dose shows the slowest recovery toward equilibrium.

It is not obvious how a decrease in the mobility of the amorphous or interfacial regions, by cross-linking between chains, should manifest itself in a significant

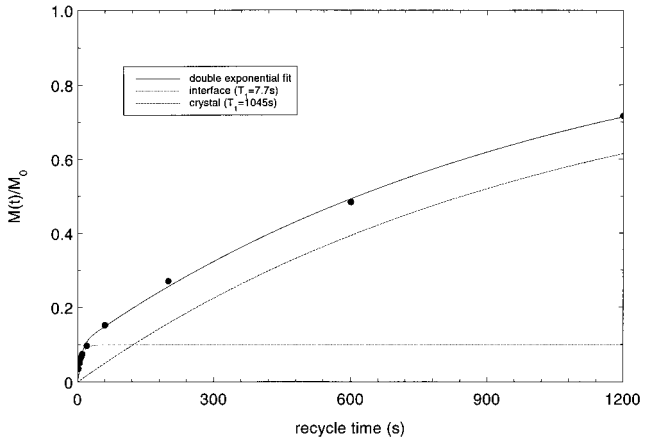

Figure 7. ^{13}C relaxation data for the unirradiated sample, fitted to a conventional two-component T_1 mechanism. The crystal region is described by a long time component, while the interfacial region is modeled with a much shorter T_1 value.

Table 2. Time Constants (T_1) and Intensities (I_0) from the Fitting of the Relaxation Data to a Double Exponential[a]

gel fraction	I_0^I (%)	T_1^I (s)	I_0^C (%)	T_1^C (s)
0	10	7.7	90	1045
0.78	9	6.2	91	1323
0.87	9	6.2	91	1724

[a] The superscripts I and C represent the intermediate and crystalline components respectively.

increase in the time scale for the crystalline spin−lattice relaxation. However, the dependence of the data can be explained if the origin of the longitudinal relaxation is molecular chain diffusion.

However, the extent to which the results can be interpreted using the classical spin−lattice relaxation model should be investigated before being rejected. As the ^{13}C longitudinal relaxation does not exhibit a single dipolar spin−lattice relaxation, the analysis has frequently involved a multiexponential model,[10,11] with the longest component empirically attributed to the major part of the crystalline lamellae. The origin of the shorter T_1 is typically associated with relaxation in the interface. To investigate whether a multiexponential model adequately represents the observed data, the approach of Cheng *et al.*[10] has been adopted. The relaxation was modeled by a double exponential, with the components assigned to the crystal and interfacial regions. The results of this fitting can be seen in Figure 7. The two-domain model, each domain with a distinct spin−lattice relaxation, provides a satisfactory model for the observed longitudinal relaxation of crystalline signal. An intermediate phase, approximately 9% of the ^{13}C crystalline signal, has a short T_1 measured in seconds. However, the dominant relaxation is an extremely long T_1, typically larger than 1000 s, which is designated as the crystalline signal.

Although the observed relaxation is adequately represented, the resultant time constants require careful consideration (Table 2). Values determined for the crystalline phase demonstrate an increase for their time scale with irradiation dose. The principal affect of electron irradiation, however, is to place cross-links between chains in the amorphous or interfacial regions of the polymer, which should not affect the mobility within the crystal. Thus, the T_1 values should remain constant, which contradicts the observed behavior.

Introduction of cross-links in the interfacial region should significantly hinder the mobility of this region, with a corresponding increase in the T_1 value. However, the T_1 time constant is observed to decrease slightly with a larger irradiation dose. So, although a multiexponential model adequately represents the relaxation data, the resultant T_1 values do not conform to the physical description of cross-linking.

Analysis of the classic spin−lattice model can be extended by calculating the correlation time, τ_R, for the motion responsible for the relaxation.[18] It is assumed in this analysis that the full $^{13}C-^{1}H$ dipolar coupling is modulated by the motion described through the correlation time. Additional motion to this molecular reorientation, e.g., a libration of the CH_2 group about the molecular axis, would correspond to an increase in the T_1 value. Thus, the correlation time, estimated in the fast motion limit, represents the minimum allowable value, while that in the slow motion regime represents the maximum. Hence, for a $T_1 \approx 1000$ s, the correlation times can be estimated for both regimes, i.e. $\tau_R \leq 1.4 \times 10^{-4}$ s or $\tau_R \geq 2.4 \times 10^{-14}$ s. Taken in conjunction with the limiting τ_R determined from the NOE measurements ($\tau_R \leq 7.6 \times 10^{-10}$), this suggest that motions with rates exceeding 1 GHz are required to account for a conventional spin−lattice relaxation time constant. Obviously, motion with these rates is unrealistic for molecular reorientation in the crystallites. This would strongly indicate that the crystal magnetization is not generated through the crystalline dipolar spin−lattice relaxation. In conjunction with the fact that the observed NOE is the same for both the crystalline and amorphous resonances, a dipolar spin−lattice mechanism can be discounted as the origin of the longitudinal relaxation. However, the hypothesis that the magnetization is transported from the crystal to the amorphous regions, where it experiences an efficient relaxation process, is consistent with the data.

Although the low natural abundance of ^{13}C isotopes suggests that the direct spin diffusion mechanism would be inefficient, the diffusion might proceed through the tightly coupled ^{1}H spin system. Spin diffusion in a dilute spin system can be modulated through an abundant spin species.[20] However, the creation of a more rigid system by cross-linking, especially at the interface, should intuitively either not affect or possibly enhance the spin diffusion, dipolar interactions being more efficient in a rigid system. However, as this is in contradiction to the data, the mechanism of magnetization transport is assigned to the solid-state diffusion of polymer chains.

Molecular Chain Diffusion. Diffusion of chain stems within the crystallites cannot be entirely independent of each other. However, a Fick's law diffusion was used with the initial and boundary conditions representing the polymer structure and its magnetization. Diffusion into a slab of thickness $2l$, where effectively all the diffusing material enters through the plane faces and a negligible amount enters through the edges was used as a model to fit the experimental data.[21] This was considered equivalent to the one-dimensional longitudinal diffusion into a crystal lamella.

The surfaces are maintained at constant concentration C_0, with initially zero concentration of diffusing substance throughout the slab. This represents the initial condition of the system, where the magnetization in the amorphous domain is fully relaxed, while the magnetization in the crystal is saturated. Diffusion of the relaxed magnetization into the slab, as polymer chains enter and leave the crystallites, is given by eq 4,

$$\frac{M(t)}{M_0} = 1 - \sum_{n=0}^{\infty} 2C_n \exp\left[-\frac{Dt}{C_n l^2}\right] \qquad (4)$$

where $C_n = 4/(2n + 1)^2\pi^2$ and D is the diffusion coefficient.

A nonlinear iterative algorithm was used to model the data to eq 4. The procedure, based on the Levenberg-Marquardt algorithm,[22] gradually modifies the search for the minimization of χ^2, the merit function, from a steepest descent approach to a quadratic procedure. An accuracy to four significant figures for the diffusion coefficient was established by using only the first 10 terms of the sum, and the appropriate limiting step. The results of the fitting are shown in Figure 6.

Unconstrained diffusion of the magnetization from the amorphous phase into the crystal satisfactorily represents the relaxation behavior of the nonirradiated polyethylene, at 60 °C. Perhaps surprisingly, the polyethylene sample irradiated at the highest dose and, hence, with the greatest number of cross-links was also adequately modeled by the equation.

Even at the highest irradiation dose the relaxation cannot be modeled by a single exponential. The inability to abstract an intrinsic dipolar spin−lattice relaxation from the highly cross-linked samples does not indicate its absence. As the diffusion equation is essentially a sum of exponentials, the conventional dipolar mechanism for relaxation of the crystal magnetization is contained within that sum. Therefore, the diffusion coefficients obtained, although reflecting the longitudinal relaxation, may not accurately represent the actual displacement of the polymer chains.

If it is assumed that the introduction of a single cross-link inferred insolubility upon the polymer, then the gel fraction may be interpreted as the fraction of chains with at least a single cross-link to another chain.[23] A high gel fraction may be obtained with a relatively small number of cross-links, especially as cross-links were formed on the crystal fold surfaces. If these cross-links connect chains between loose fold surfaces, the chain stems may still exhibit a relatively large displacement into the crystal before the cross-links impede its further progress.

Table 3 gives the diffusion coefficients calculated from the fits to eq 4. Analysis of the diffusion coefficients infers important information about the molecular diffusion process. Comparison of D measured over the period of the chains initial displacement, i.e., $\tau \leq 20$ s, and over the longer time, i.e., $\tau \leq 1200$ s, demonstrate a dependence on the distance the chains have diffused.

In the initial stages of diffusion, it is unlikely that many of the constraints are important, as the longitudinal relaxation is dominated by the free diffusion of the polymer chains. Constraints, including chain ordering, entanglements, and cross-links, become more significant as the diffusion continues. At the long times,

Table 3. Diffusion Coefficients Obtained from the Fits to Eq 5, for the Complete Range of Data and the Shortened Period

	D ($nm^2 \cdot s^{-1}$)	
gel fraction	$\tau \leq 20$ s	$\tau \leq 1200$ s
0	0.0421	0.0330
0.78	0.0377	0.0247
0.87	0.0350	0.0183

the constraints severely hinder the molecular chain diffusion, as the portion of chains, which were closest to the core of the crystal, become virtually locked within the crystallite.

The diffusion coefficients demonstrate a systematic reduction in value with increased irradiation dose. This behavior is seen for D, when measured over the full range of experimental times but also over the initial period of chain diffusion. As the only difference between samples was the introduction of more topological constraints, in the form of cross-links, molecular chain diffusion becomes more impeded with irradiation dose. It is worth noting that the diffusion coefficients we obtain are consistent with those of Schmidt-Rohr and Spiess,[8] who used an entirely different (Monte Carlo) analytical approach. Also, it is interesting to note that Colquhoun and Packer,[7] in a study of branched polyethylenes, also invoked the idea of molecular chain diffusion contributing to the ^{13}C relaxation process. Their diffusion coefficients are also broadly comparable to this work, allowing for the differences in polymer morphology and method of data analysis.

Conclusions

A progressive saturation pulse sequence has been used to investigate the ^{13}C longitudinal relaxation on a series of polyethylene samples which had experienced various electron irradiation treatments. The samples were shown to exhibit various degrees of cross-linking, through measurement of the gel fraction.

Although the relaxation data were adequately modeled by a multicomponent spin−lattice relaxation, the resultant T_1 values did not conform to the physical model of a cross-linked polymer. An increase in the T_1 value of the crystalline signal was observed with an increase in cross-link density, while the short T_1, associated with the interface, decreased. As irradiation forms cross-links at the fold surface of the lamellae, a conventional dipolar spin−lattice relaxation model was contradicted by the physical interpretation of its mobility. A molecular diffusion model, however, is consistent with the data.

Previous experimental evidence has demonstrated the possibility for the displacement of chains within *n*-alkane crystals. On a macroscopic scale, the transverse and longitudinal migration of paraffin chains in the crystal state has been observed by direct optical observation[24] and X-ray diffraction.[25] However, whether this movement could result in the principal mechanism for the ^{13}C longitudinal relaxation was not apparent.

Isolated polyethylene chains in organic inclusion compounds strongly indicated the possibility for the displacement of chains in polymer crystals.[26] ^{2}H NMR line shapes and relaxation experiments demonstrated that the principal motion was a high-frequency libration of the C−C bond. This motion, equivalent to the chain jump mechanism previously observed in polyethylene,[9,27,28] caused a fluctuation in the position of the chain relative to its long axis.

Whereas existing ^{13}C longitudinal relaxation data has largely been interpreted through a conventional dipolar spin−lattice model, the relaxation was established as the transport of magnetization, through molecular chain diffusion, into the amorphous phase. Consequently a re-evaluation of theories which draw on such data may be required, with the measurement of molecular chain diffusion stimulating new investigations in the field of ordering, structure and dynamics in semicrystalline polymers. A future publication will consider the effect of lamellar thickness and morphology on the chain diffusion.

Acknowledgment. We thank Dr. M. J. Taylor of the BP Research Centre, Sunbury-on-Thames, U.K., for his advice on various aspects of the NMR experiments.

References and Notes

(1) VanderHart, D. L. *Macromolecules* **1979**, *12*, 1232−1235.
(2) Schröter, B.; Posern, A. *Makromol. Chem* **1981**, *182*, 675−680.
(3) Schröter, B.; Posern, A. *Makromol. Chem., Rapid Commun.* **1982**, *3*, 623−628.
(4) Axelson, D. E. *J. Polym. Sci., Polym. Phys.* **1982**, *20*, 1477−1435.
(5) Kaji, A.; Yamanaka, A.; Murano, M. *Polym. J.* **1990**, *22*, 893−900.
(6) Axelson, D. E.; Mandelkern, L.; Popli, R.; Mathieu, P. *J. Polym. Sci., Polym. Phys.* **1983**, *21*, 2319−2335.
(7) Colquhoun, I. J.; Packer, K. J. *Br. Polym. J.* **1987**, *19*, 151−163.
(8) Schmidt-Rohr, K.; Spiess, H. W. *Macromolecules* **1991**, *24*, 5288−5293.
(9) Fröhlich, H. *Proc. Phys. Soc.* **1942**, *54*, 442-.
(10) Cheng, J.; Fone, M.; Reddy, V. N.; Schwartz, K. B.; Fisher, H. P.; Wunderlich, B. *J. Polym. Sci., Polym. Phys.* **1994**, *32*, 2683−2693.
(11) Kitamaru, R.; Horii, F.; Zhu, Q.; Bassett, D. C.; Olley, R. H. *Polymer* **1994**, *35*, 1171−1181.
(12) Patel, G. N.; Keller, A. *J. Polm. Sci., Polym. Phys. Ed.* **1975**, *13*, 303−321.
(13) Klein, P. G.; Woods, D. W.; Ward, I. M. *J. Polym. Sci., Polym. Phys. Ed.* **1987**, *25*, 1359−1379.
(14) Klein, P. G.; Gonzalez-Orozco, J. A.; Ward, I. M. *Polymer* **1991**, *32*, 1732−1736.
(15) Becker, E. D.; Ferretti, J. A.; Gambhir, P. N. *Anal. Chem.* **1979**, *51*, 1413−1420.
(16) Neuhaus, D.; Williamson, M. P. *The Nuclear Overhauser Effect in Structural and Conformational Analysis*; VCH Publishers: New York, 1989; Chapter 1-2.
(17) Noggle, J. H.; Schirmer, R. E. *The Nuclear Overhauser Effect: Chemical Applications*, Academic Press, New York, 1971, Chapter 1.
(18) Doddrell, D.; Glishko, V.; Allerhand, A. *J. Chem. Phys.* **1972**, *56*, 3683−3689.
(19) Robertson, M. B. Ph.D. Thesis, University of Leeds, 1996; chapter 4.
(20) Robyr, P.; Tomaselli, M.; Straka, J.; Grob-Pisano, C.; Suter, U. W.; Meier, B. H.; Ernst, R. R. *Mol. Phys.* **1995**, *84*, 995−1020.
(21) Crank, J. *The Mathematics of Diffusion*; Clarendon Press: Oxford, England, 1975; Chapter 4.
(22) Marquardt, D. W. *J. Soc. Ind. Appl. Math.* **1963**, *11*, 431−441.
(23) Klein, P. G.; Ladizesky, N. H.; Ward, I. M. *J. Polym. Sci., Polym. Phys. Ed.* **1986**, *24*, 1093−1113.
(24) Yamamoto, T.; Nozaki, K. *Polymer* **1995**, *36*, 2505−2510.
(25) Ungar, G.; Keller, A. *Colloid Polym. Sci.* **1979**, *257*, 90−94.
(26) Schilling, F. C.; Amundson, K. R.; Sozzani, P. *Macromolecules* **1994**, *27*, 6498−6502.
(27) Olf, H. G.; Peterlin, A. *J. Polym. Sci., A-2* **1970**, *8*, 771−789.
(28) Folkes, M. J.; Ward, I. M. *J. Mater. Sci.* **1971**, *6*, 582−596.

MA9708712